Nanoscale Res Lett (2010) 5:1675–1681
DOI 10.1007/s11671-010-9694-y

NANO EXPRESS

Formation of ZnO Micro-Flowers Prepared via Solution Process and their Antibacterial Activity

Rizwan Wahab · Young-Soon Kim · Amrita Mishra · Soon-Il Yun · Hyung-Shik Shin

Received: 22 April 2010 / Accepted: 1 July 2010 / Published online: 1 August 2010

Abstract This paper presents the fabrication and characterization of zinc oxide micro-flowers and their antibacterial activity. The micro-flowers of zinc oxide composed of hexagonal nanorods have been prepared via solution process using precursor zinc acetate di-hydrate and sodium hydroxide in 3 h of refluxing time at ~90°C. The antibacterial activities of grown micro-flowers were investigated against four pathogenic bacteria namely *S. aureus, E. coli, S. typhimurium and K. pneumoniae* by taking five different concentrations (5–45 μg/ml) of ZnO micro-flowers (ZnO-MFs). Our investigation reveals that at lowest concentration of ZnO-MFs solution inhibiting the growth of microbial strain which was found to be 5 μg/ml for all the tested pathogens. Additionally, on the basis of morphological and chemical observations, a chemical reaction mechanism of ZnO-MFs composed of hexagonal nanorods was also proposed.

Keywords *E. coli* · *S. aureus* · X-ray diffraction pattern · ZnO micro-flowers and antibacterial activity

Rizwan Wahab and Young-Soon Kim contributed equally to this work.

R. Wahab · Y.-S. Kim · H.-S. Shin (✉)
Energy Materials & Surface Science Laboratory, Solar Research Center, School of Chemical Engineering, Chonbuk National University, Jeonju 561-756, Republic of Korea
e-mail: hsshin@chonbuk.ac.kr

A. Mishra · S.-I. Yun
Department of Food Science and Technology, College of Agriculture and Life Sciences, Chonbuk National University, Jeonju 561-756, Republic of Korea

Introduction

Human beings are very commonly infected by microorganisms in the living environment, which sometimes results in illness and other health hazards. Microorganisms harmful to human beings are termed as pathogens. In the recent past, due to the emergence and increase of such pathogenic strains resistant to multiple antibiotics [1, 2] and the continuing emphasis on health care costs, many researchers have tried to develop new, effective antimicrobial reagents free of resistance and cost. The antimicrobial activity is known to be a function of the surface area in contact with the microorganisms. A larger surface area (as in case of nanoparticles) ensures a broad range of probable reactions with bio-organics present on the cell surface, as well as environmental and organic species [3]. Metal nanoparticles, which have high specific surface area and high fraction of surface atoms, have been studied extensively owing to their unique antibacterial activity [4–6]. Much research has also been done to study the antibacterial activity of metal oxide powders and nanoparticles [7–13]. In this regard, ZnO nanoparticles have received increasing attention over the years. ZnO is known for its stability under harsh processing conditions and is also listed as GRAS i.e., generally regarded as safe for human beings [14, 15]. The above fact is exemplified by previous studies where ZnO nanoparticles seem to have relative toxicity to bacteria but exhibit minimal effect on human cells [13, 16]. The antibacterial activity of ZnO powder and nanoparticles has been effectively studied against some of the multiresistant pathogens such as *Staphylococcus aureus* and *Escherichia coli* [13, 17]. Antimicrobial properties of polymer coatings with ZnO tetra pods have also been observed [13]. Although the antibacterial activity of the ZnO nanoparticles has been

well established, still the exact mechanism underlying and it is not completely understood. Over the years, several mechanisms have been proposed by many researchers in this context. In this paper, we report the fabrication of zinc oxide micro-flowers composed of nanorods (referred to as ZnO-MFs) using precursor zinc acetate di-hydrate and the source material of flower sodium hydroxide via solution process at a very low refluxing ($\sim$90°C) temperature for 3 h. The structure, phase and morphology of synthesized product were analyzed by the standard characterization techniques. On the basis of characterization, a formation mechanism for the ZnO-MFs has also been proposed. Additionally, we have tried to investigate the antibacterial activity of ZnO-MFs against four pathogenic bacteria such as *Staphylococcus aureus, Escherichia coli, Salmonella typhimurium and Klebsiella pneumoniae.* An attempt is also made to find the minimum inhibitory concentration (MIC) of the MFs capable of inhibiting the growth of the above pathogenic strains.

Experimental

Material Synthesis

Micro-flowers of zinc oxide composed of hexagonal nanorods were fabricated by the use of precursor zinc acetate di-hydrate ($Zn(CH_3COO)_2{\cdot}2H_2O$) and sodium hydroxide (NaOH) (sigma–aldrich chemical corporation). For this, in a typical experiment, 0.3 M of zinc acetate di-hydrate was dissolved in 100 ml of distilled water with 3 M concentration of sodium hydroxide. White-colored solution was appeared for few seconds but after 2–3 min, it was disappeared. The obtained solution was stirred for 10 min for the complete dissolution. Colorless solution of zinc acetate di-hydrate and sodium hydroxides pH was measured by the expandable ion analyzer (EA 940, Orian made from UK) and it was found that the pH of the solution was reached 12.6. After the complete dissolution, the mixture was transferred to the three-necked refluxing pot and refluxed at 90°C for 3 h. The white precipitate was observed when the temperature raises at 90°C but for the complete precipitation, the solution was refluxed for 3 h. The refluxing temperature was measured and controlled by k-type thermocouple with a PID temperature controller. After refluxing, the white powder was washed with methanol several times and dried at room temperature. The obtained as grown powder was examined in terms of their structural and chemical properties.

Characterization of Synthesized Materials

The morphological observations of the white powders were made by a FESEM and TEM at room temperature. For SEM observation, the powder was uniformly sprayed on carbon tape. In order to avoid charging while observation, the powder was coated by thin osmium oxide (OsO_4) for 5 s. For the transmission electron microscopic measurement, powder was sonicated in an ethanol for 10 min by a locally supplied ultrsonicator (40 kHz, Mujigae Seong Dong, Korea) and then a copper grid was dipped in the solution and dried at room temperature. After drying, sample was analyzed at 200 kV whereas the bacteria and bacteria with ZnO-MFs were analyzed via transmission electron microscope (Bio-TEM) (Hitachi (H-7650 Japan, Resolution: 0.2 nm (lattice image) at 100 kV. The crystallinity and phases of white powder were characterized by an X-ray powder diffractometer (XRD) with $Cu_{K\alpha}$ radiation ($\lambda = 1.54178$Å) in the range of 20–65° with 8°/min scanning speed. Apart from these characterizations, the composition of white powder was characterized via Fourier transform infrared (FTIR) spectroscopy in the range of 4,000–400 cm^{-1}.

Antibacterial Activity of ZnO-MFs

Bactericidal activity of the ZnO-MFs was tested using the growth inhibition studies against four pathogenic microorganisms such as *Staphylococcus aureus* KCCM 11256, *Escherichia coli* KCCM 11234, *Salmonella typhimurium* KCCM 11862 and *Klebsiella pneumoniae* KCCM 35454. All the above strains were purchased from Korean Culture Centre of Microorganisms (KCCM). For the antibacterial test, sterile 250-ml Erlenmeyer flasks, each containing 100 ml of nutrient broth medium and the desired amount of ZnO-MFs, were inoculated with 1 ml of freshly prepared bacterial suspension in order to maintain the initial bacterial concentration in the same range in all the flasks. The flasks were then incubated in a rotary shaker at 150 rpm at 37°C. The bacterial growth was monitored at regular intervals for 24 h by measuring the increase in absorbance at 600 nm in a spectrophotometer (Shimadzu, UV-2550).The experiments also included a control flask containing only media and bacteria devoid of ZnO-MFs.

Results and Discussion

Structural Characterization

Figure 1a shows the X-ray diffraction pattern of grown ZnO-MFs prepared at above parameters. The spectra clearly shows the diffraction peaks in the pattern indexed as the zinc oxide with lattice constants $a = 3.249$ and $c = 5.206$ Å, and well matched with the available Joint Committee on Powder Diffraction Standards (JCPDS 36-1451).There is no other peak related to impurities were

detected in the spectra within the detection limit of the X-ray diffraction, which further confirms that the synthesized powders are pure ZnO. The general morphology of the grown ZnO-MFs prepared at above conditions were observed via FE-SEM and presented in Fig. 1b–d. From low magnification FE-SEM images (Fig. 1b–c of ZnO-MFs, the full micro-flowers (MFs) can be seen. The individual growth unit of micro-flower is evident at higher magnification (Fig. 1d). The full array of each micro-flowers (MF) shaped structure is in the range of 2–3μm. From Fig. 1d, the high magnification images of the micro-flowers (MFs) reveals that the flower structures are made up by the accumulation of several hundreds of small hexagonal nanorods. The diameter of each nanorods is in the range of 150–200 nm whereas length goes up to 2μm. From FESEM images we can easily observe that nanorods are in hexagonal shape with pointed tip morphology. The individual ZnO nanorods are joining with other nanorods as like leaf of flower and forming wider bases for the complete flower-shaped structure.

Furthermore, the morphology of grown ZnO-MFs was again characterized via transmission electron microscopy (TEM). Figure 1e shows the low-magnification image of grown ZnO-MFs, whose base diameter is ~2–3 μm, whereas the individual nanorod exhibits ~150–200 nm diameter and it is clearly constant with the FESEM observations (Fig. 1d), revealing that the formed MFs are made up with the accumulation of small hexagonal shaped zinc oxide nanorods. Additionally, SAED (selected area electron diffraction) pattern is defining the growth direction of the nanorods and confirming that the obtained nanostructures are single crystalline with the wurtzite phase and preferentially grown along the [0001] direction. Figure 1f shows the HR-TEM (high-resolution transmission electron

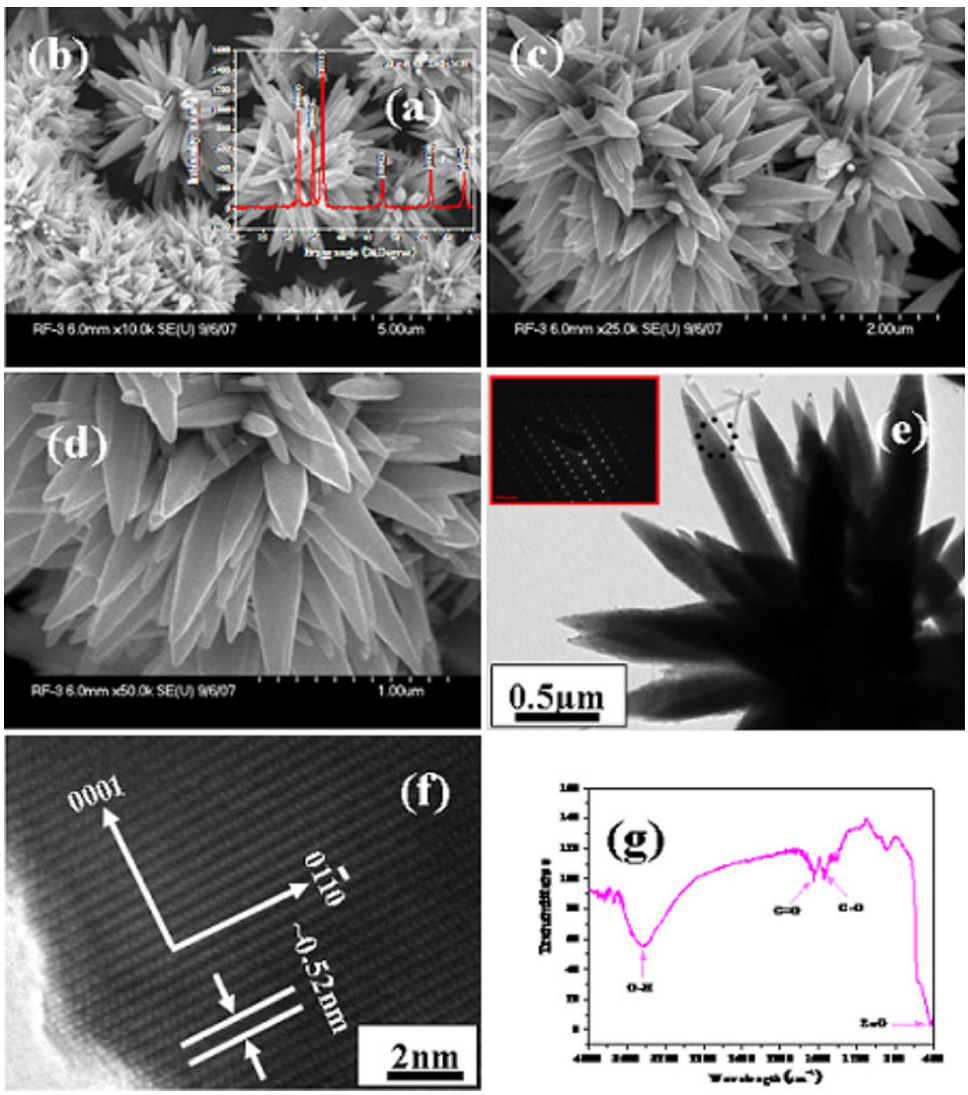

Fig. 1 **a** shows the typical X-ray diffraction pattern of grown zinc oxide micro-flowers (ZnO-MFs) composed of hexagonal nanorods, **b**, **c** shows the low magnification and **d** shows the high magnification FESEM images of ZnO-MFs **e** shows the low magnification TEM image of ZnO-MFs and inset presents the SAED (selected area electron diffraction) pattern of grown ZnO nanorods whereas **f** presents the HR-TEM image and it shows that the lattice difference between two fringes is ~0.52 nm **g** presents the typical FTIR spectrum of grown ZnO-MFs

microscopy) image of circled area of hexagonal nanorods (Fig. 1e). From the HR-TEM image we can understand that the distant of lattice fringes between two adjacent planes which is ~0.52 nm and it is equal to the lattice constant of ZnO. The observed lattice distance from HR-TEM image again indicating that the obtained nanorods of flower-shaped morphology have wurtzite hexagonal phase and are preferentially grown along the *c*-axis [0001] direction (Fig. 1f).

The functional or composition quality of the synthesized product was analyzed by the FTIR spectroscopy. Figure 1g shows the FTIR spectrum which was acquired in the range of 400–4,000 cm^{-1}. The band at 430 cm^{-1} is correlated with zinc oxide [18]. Whereas the bands at 3,200–3,600 cm^{-1} corresponds to the O–H mode of vibration and the starching mode of vibration of C = O and C–O are observed at 1,638 and 1,506 cm^{-1}, respectively [19, 20]. The formation of ZnO is consisted of the X-ray diffraction pattern and FTIR data (Fig. 1a) [21].

Chemical Reaction Mechanism of Synthesized Zinc Oxide Micro-Flowers (ZnO-MFs)

Based on the above findings, a simple reaction mechanism is proposed for the zinc oxide micro-flowers (ZnO-MFs) composed of nanorods via solution process. When zinc acetate di-hydrate ($Zn(CH_3COO)_2{\cdot}2H_2O$) was dissolved under continuous stirring in double deionized water, and to this solution alkali sodium hydroxide was pored, it forms a white suspension for few seconds, but for the complete dissolution it was stirred for 10 min without precipitate at pH ~ 12.6. After the dissolution, the solution of zinc acetate di-hydrate ($Zn(CH_3COO)_2{\cdot}2H_2O$) and sodium hydroxide was transferred to the refluxing pot and refluxed at 90°C. We presume that in the refluxing pot, as the temperature raises, precursor zinc acetate di-hydrate ($Zn(CH_3COO)_2{\cdot}2H_2O$) and sodium hydroxide react as below:

$$Zn(CH_3COO)_2{\cdot}2H_2O + 2NaOH \rightarrow Zn(OH)_2 + 2CH_3COONa + 2H_2O \quad (1)$$

$$Zn(OH)_2 + 2H_2O \rightarrow \left[Zn(OH)_4^{2-}\right]^{2+} + 2H^+ \quad (2)$$

$$\left[Zn(OH)_4^{2-}\right]^{2+} \rightarrow ZnO + H_2O + 2OH^- \quad (3)$$

The fabrication/growth mechanism of micro-flowers (ZnO-MFs) composed of hexagonal nanorods is based on the initial precipitation of $Zn(OH)_2^{2+}$ and $[Zn(OH)_4^{2-}]^{2+}$ in an aqueous solution of refluxing pot. In the solution of zinc acetate di-hydrate and sodium hydroxide, as the pH value of the solution is increases, the number of hydroxyl ions (OH^- ion) increases. The complex $Zn(OH)_2^{2+}$ and $[Zn(OH)_4^{2-}]^{2+}$ generally generated in an aqueous solution at above pH = 9 and it is expected that the $[Zn(OH)_4^{2-}]^{2+}$ is a growth unit of wurtzite ZnO [22]. As we know that the $Zn(OH)_2$ precipitate is more soluble than ZnO precipitates [18], the $Zn(OH)_2$ continuously produces Zn^{2+} and OH^- ions, which form the ZnO nuclei. ZnO behaves as polar crystal, where zinc and oxygen atoms are arranged alternatively along the *c*-axis and the top surface-plane is a Zn-terminated (0001) plane while the bottom surface is oxygen-terminated (000$\bar{1}$) plane. The Zn-(0001) is catalytically active while the O-(000$\bar{1}$) is inert [23]. Furthermore, the growth habit depends upon the growth velocities of different planes in the ZnO crystal. According to laudise and Ballman reported that the higher the growth rate, the faster the disappearance of a plane, which leads to the pointed shape on the end of the *c*-axis [24]. In ZnO, the growth velocities of the ZnO plane in different directions are $[0001] > [01\bar{1}\bar{1}] > [01\bar{1}0] > [01\bar{1}1] > [000\bar{1}]$, under hydrothermal conditions [24]. Therefore, the (0001) plane, the plane with the most rapid growth rate, disappears which leads to the pointed shape at the end of the {0001} direction. Moreover, the (000$\bar{1}$) plane has the slowest growth rate, which leads to the flat plane at the other shape end. In our synthesized nanostructures, all the observed nanorods have pointed tips with wide bases, which is consistent with the ideal growth habit of ZnO crystals [25, 26].

Antibacterial Activity of Synthesized Zinc Oxide Micro-Flowers (ZnO-MFs)

For studying the antibacterial effect, five different concentrations (5, 15, 25, 35 and 45 μg/ml) of the ZnO-MFs have been taken as can be seen in Figs. 2, 3, 4, 5. It has been observed that the minimum inhibitory concentration (MIC) defined as the lowest concentration of the ZnO-MFs solution that inhibits growth of the microbial strain is found

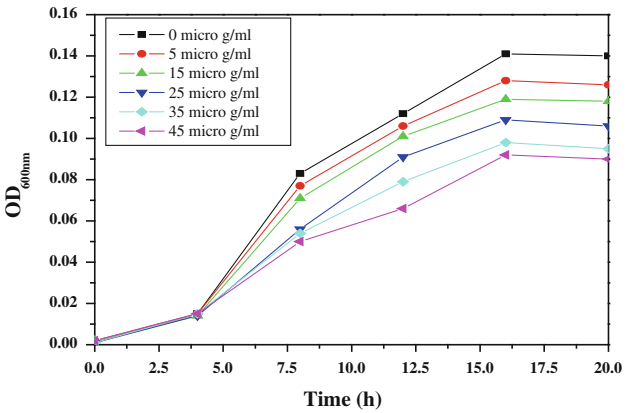

Fig. 2 Bacterial growth curve of *E. coli* with increasing concentration of ZnO-MFs

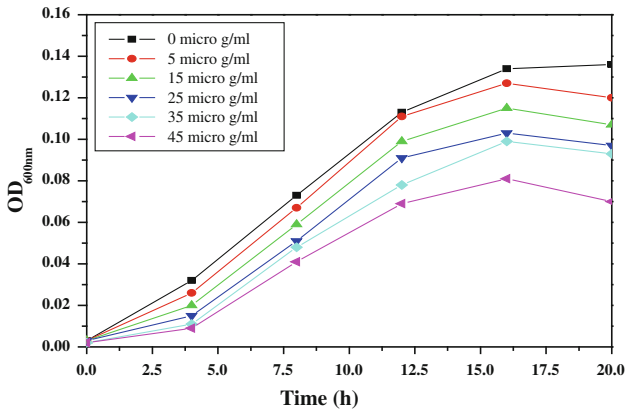

Fig. 3 Bacterial growth curve of *K. pneumoniae* with increasing concentration of ZnO-MFs

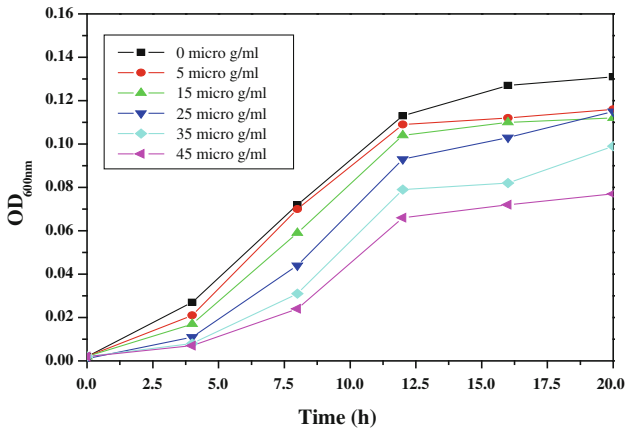

Fig. 4 Bacterial growth curve of *S. aureus* with increasing concentration of ZnO-MFs

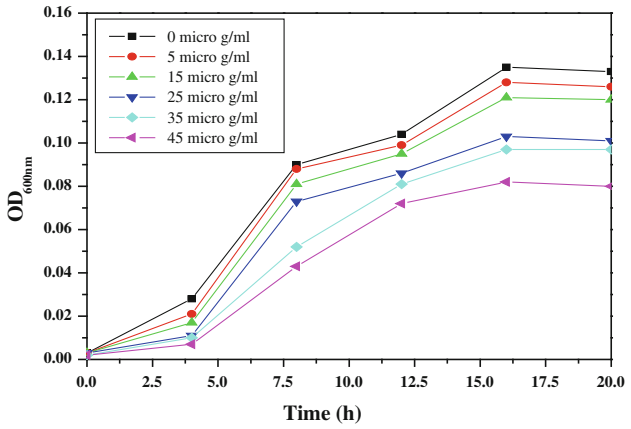

Fig. 5 Bacterial growth curve of *S. typhimurium* with increasing concentration of ZnO-MFs

to be 5 μg/ml for all the pathogens. However, in case of all the four microbial strains, it has been seen that with the increase in concentration of ZnO-MFs solution, the growth of inhibition has also been increased. Noticeable difference in growth rate has been noticed for all the organisms after 3–4 h of incubation with ZnO-MFs solution whereas in case of *E. coli*, difference in the growth curve can be observed after 5 h of incubation (Fig. 2). The highest concentration of the ZnO-MFs solution (45 μg/ml) has been found to strongly inhibit the growth of all the pathogenic strains tested. In case of all the pathogen, the logarithmic growth phase is found to be prolonged starting from 5 h of incubation of the organisms up to more than 15 h of incubation. In case of *S. aureus*, the log phase can be seen up to 20 h of incubation of the organism with different concentration of ZnO-MFs as well as in control (Fig. 3). ZnO-MFs have showed effective antibacterial activity against both gram-positive and gram-negative bacterial strains. The results obtained in our study indicate that the inhibitory efficacy of ZnO-MFs is very much dependant on its chosen concentration, size and shape which is similar to earlier findings [13, 16]. Overall, the preliminary findings suggest that the ZnO-MFs can be used externally to control the spreading of bacterial infections. The cell wall of most pathogenic bacteria is composed of surface proteins for adhesions and colonization and components such as polysaccharides and teichoic acid that protect against host defenses and environmental conditions [27]. It has been reported that certain long-chain polycations coated onto the surfaces can efficiently kill on contact both gram-positive and gram-negative bacteria [28, 29]. The above studies have indicated that families of unrelated hydrophobic groups are equally efficient at killing bacteria. Therefore, it is expected that ZnO-MFs may be used externally as antibacterial agents as surface coatings on various substrates to prevent microbial growth leading to the formation of biofilms in medical devices and other equipments.

The mechanism/relation between the bacteria and ZnO-MFs and its antibacterial activity have been further elucidated via Bio-Transmission electron microscopy (Bio-TEM) images. Figures 6, 7 show the TEM images of the tested bacteria *E. coli, K. pneumoniae, S. typhimurium* and *S. aureus,* after treatment with zinc oxide micro-flowers (ZnO-MFs). Figures 6a, b show *E. coli* and *E. coli* with ZnO-MFs at MIC of zinc oxide sample after 18 h of incubation. The inset picture (Fig. 6b) is showing the unit morphology of ZnO-MFs after the interaction of *E. coli.* In case of *E. coli,* it is clear from the image that the nanorods have attached at first to the outer membrane of the cell and the nanorods have further entered into the cell completely, which might have lead to cell death. Similar result has been observed with *K. pneumoniae* (Fig. 6c, d). In case of *S. typhimurium* and *S. aureus* (Fig. 7a–d), leakage of internal contents of the cell has been observed, which is clear from the images (Fig. 7b, d). However, the flowers composed of nanorods have attached to the outer wall of the

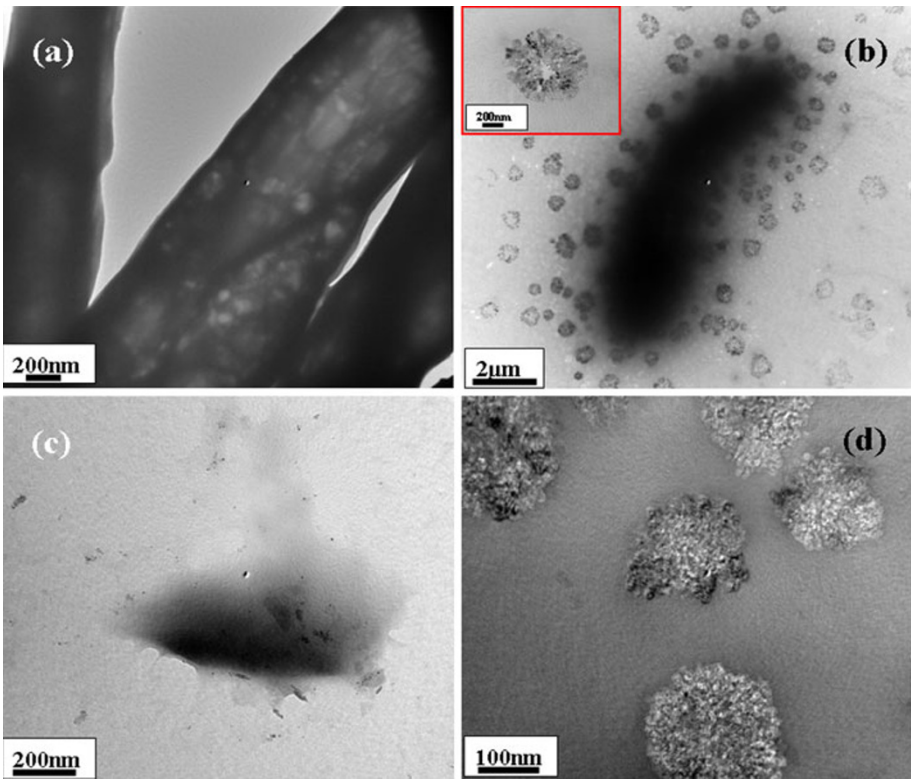

Fig. 6 Typical Bio-TEM images of: **a** *E. coli*, **b** and *inset* ZnO-MFs with *E. coli* at different stages, **c** *K. pneumoniae*, **d** ZnO-MFs with *K. pneumoniae*

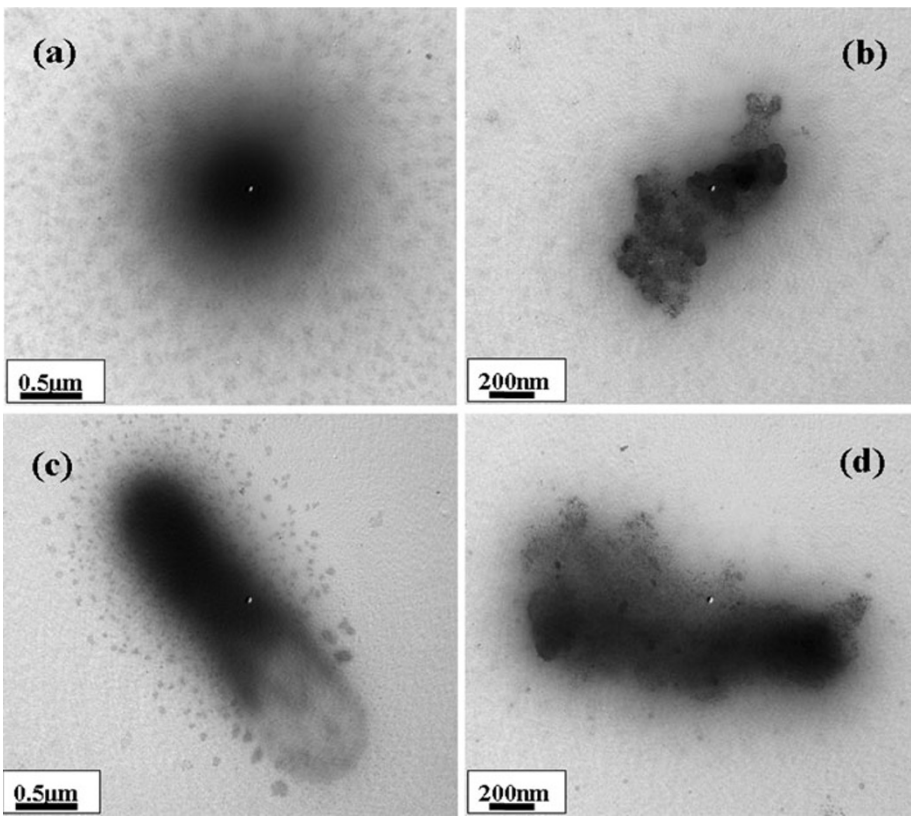

Fig. 7 Typical Bio-TEM of: **a** *S. typhimurium*, **b** *S. typhimurium* with ZnO-MFs, **c** *S. aureus* and **d** ZnO-MFs with *S. aureus*

cell in the beginning and further they have entered to the inner wall of the cell leading to disruption of the internal contents of the cell and as a result the cells have been deformed leading to disorganization and leakage. Further conclusive studies are needed to conclude the relation of antibacterial activity with ZnO-MFs as altered cell membrane permeability and intracellular metabolic system in bacterial cells caused by ZnO-MFs cannot be visualized by Bio-TEM images [30]. Although cellular internalization and membrane disruption have been observed in the TEM images, any change in the morphology of the cells cannot be predicted from the images. Although possible mechanisms have been proposed in earlier reports [13, 16], still the exact mechanism underlying the antibacterial activity of the ZnO-MFs remains to be understood. Further study and research are needed to find out the exact mechanism of membrane damage and lyses of bacterial cells caused due to ZnO-MFs.

Conclusions

We have presented here the fabrication of zinc oxide micro-flowers and their antibacterial activity using zinc acetate di-hydrate ($Zn(CH_3COO)_2{\cdot}2H_2O$) and sodium hydroxide (NaOH) via solution process. The morphology of the grown micro-flowers (MFs) was characterized via microscopic (FESEM and TEM) studies; on the other hand, the crystallinity and compositional study were analyzed via X-ray diffraction pattern and FTIR spectroscopy. The study of antibacterial activity with zinc oxide micro-flowers (ZnO-MFs) revealed that the cell membrane as well as cytoplasm of bacteria was damaged during the incorporation of MFs. However, at this time, it is difficult to explain why such phenomenon is observed. Further studies are in progress to conclude the relation of antibacterial activity with ZnO-MFs.

Acknowledgments We acknowledge the support received from KOSEF (Korea Science and Engineering Foundation) research grant no. R01-2007-000-20810-0 is fully acknowledged. We would also like to thank Mr. Kang Jong-Gyun, Center for University-wide Research Facilities, Chonbuk National University for his cooperation in Transmission Electron Microscopy (TEM) observations and the KBSI (Korea Basic Science Institute), Jeonju branch, for letting us use their FESEM facility.

References

1. U. Desselberger, J. Infect. **40**, 3 (2000)
2. L.E. Hancook, M.S.Gilmore, V.A. Fischetti, R.P.Novick, J.J. Ferretti, D.A. Portnoy, J.I. Rood (eds.) (ASM Press, Washington DC, 2000)
3. P. Holister, J.W. Weener, C.V. Romas, T. Harper, *Nanoparticles. Technology white papers 3* (Scientific Ltd, London, 2003)
4. F. Furno, K.S. Morley, B. Wong, B.L. Sharp, P.L. Arnold, S.M. Howdle, R. Bayston, P.D. Brown, P.D. Winship, H.J. Reid, J. Antimicrob. Chemother. **54**, 1019 (2004)
5. N. Ciofi, L. Torsi, N. Ditaranto, L. Sabatini, P.G. Zambonin, G. Tantillo, L. Ghibelli, M.D. Alessio, T. Bleve-Zacheo, E. Traversa, Appl. Phys. Lett **85**, 2417 (2004)
6. N. Ciofi, L. Torsi, N. Ditaranto, G. Tantillo, L. Ghibelli, L. Sabatini, T. Bleve-Zacheo, M.D. Alessio, P.G. Zambonin, E. Traversa, Chem. Mater **17**(21), 5255 (2005)
7. J. Sawai, T. Yoshikawa, J. Appl. Microbiol. **96**, 803 (2004)
8. L. Huang, D.Q. Li, Y.J. Lin, M. Wei, D.G. Evans, X. Duan, J. Inorg. Biochem. **99**, 986 (2005)
9. W.A. Daoud, J.H. Xin, Y.H. Zhang, Surf. Sci. **599**(1–3), 69 (2005)
10. O.B. Koper, J.S. Klabunde, G.L. Marchin, K.J. Klabunde, P. Stoimenov, L. Bohra, Curr. Microbiol. **44**, 49 (2002)
11. J. Sawai, J. Microbiol. Methods **54**, 177 (2003)
12. T. Xu, C.S. Xie, Prog. Org. Coat. **46**, 297 (2003)
13. R. Brayner, R. Ferrari-Illiou, N. Briviois, S. Djediat, M.F. Benedetti, F. Fievet, Nano Lett. **6**, 866 (2006)
14. P.K. Stoimenov, R.L. Klinger, G.L. Marchin, K.J. Klabunde, Langmuir **18**, 6679 (2002)
15. G. Fu, P.S. Vary, C.T. Lin, J. Phys. Chem. **109**, 8889 (2005)
16. L.L. Zhang, Y.H. Jiang, Y.L. Ding, M. Pvey, D. York, J. Nanopart. Res. **9**, 479 (2007)
17. O. Yamamoto, Int. J. Inorg Mater. **3**, 643 (2001)
18. R. Wahab, S.G. Ansari, Y.S. Kim, H.K. Seo, G.S. Kim, G. Khang, H.S. Shin, Mater. Res. Bull. **42**, 1640 (2007)
19. R. Wahab, S.G. Ansari, Y.S. Kim, H.K. Seo, H.S. Shin, Appl. Surf. Sci. **253**, 7622 (2007)
20. R. Wahab, S.G. Ansari, Y.S. Kim, G. Khang, H.S. Shin, Appl. Surf. Sci. **254**, 2037 (2008)
21. N. Lepot, M.K.V. Bael, H.V.D. Rul, J.D. Haen, R. Peeters, D. Franco, J. Mullens, Mater. Lett. **61**, 2624 (2007)
22. W.J. Li, E.W. Shi, W.Z. Zhong, Z.W. Yin, J. Cryst. Growth **203**, 186 (1999)
23. P.X. Gao, Z.L. Wang, J. Phys. Chem. B. **108**, 7534 (2004)
24. R.A. Laudise, A.A. Ballman, J. Phys. Chem. **64**, 688 (1960)
25. R. Wahab, Y.S. Kim, H.S. Shin, Mater. Trans. **8**, 2092 (2009)
26. R. Wahab, S.G. Ansari, H.K. Seo, Y.S. Kim, E.K. Suh, H.S. Shin, Solid State Sci. **11**, 439 (2009)
27. W.W. Navarre, O. Schneewind, Microbiol. Mol. Biol. Rev. **63**, 1–174 (1999)
28. J.C. Tiller, C.J. Liao, K. Lewis, A.M. Klibanov, Proc. Natl. Acad. Sci. USA **98**, 5981–5985 (2001)
29. V. Berry, A. Gole, S. Kundu, C.J. Murphy, R.F. Saraf, J. Am. Chem. Soc. **127**, 17600 (2005)
30. M. Roselli, A. Finamore, I. Garaguso, M.S. Britti, E. Mengheri, J. Nutr. **133**, 4077–4082 (2003)